OPEN ACCESS
IOP Publishing
Journal of Physics A: Mathematical and Theoretical
J. Phys. A: Math. Theor. **53** (2020) 275202 (20pp)
https://doi.org/10.1088/1751-8121/ab91d6

Quantum metric statistics for random-matrix families

M V Berry[1,3] **and Pragya Shukla**[2]

[1] H H Wills Physics Laboratory, Tyndall Avenue, Bristol BS8 1TL, United Kingdom
[2] Department of Physics, Indian Institute of Technology, Kharagpur, India

E-mail: asymptotico@bristol.ac.uk and shukla@phy.iitkgp.ernet.in

Received 3 April 2020, revised 6 May 2020
Accepted for publication 11 May 2020
Published 15 June 2020

Abstract

The quantum metric tensor G_{ij} for parameterised families of quantum states, in particular the trace $G = \mathrm{tr}G_{ij}$, depends on the symmetry of the system (e.g. time-reversal), and the dimension N of the underlying matrices. Modelling the families by the stationary Gaussian ensembles of random-matrix, theory, we calculate the probability distribution of G, exactly for $N = 2$, and approximately for $N = 3$ and $N \to \infty$. Codimension arguments establish the scalings of the distributions near the singularities at $G \to \infty$ and $G = 0$, near which asymptotics gives the explicit analytic behaviour. Numerical simulations support the theory.

Keywords: random-matrix, quantum statistics, codimension

(Some figures may appear in colour only in the online journal)

1. Introduction

There is continuing interest, experimental [1] and theoretical [2–6], in the metric describing distances between quantum states [7]. For a family of states labelled by a parameter $\boldsymbol{r}$, the distance between neighbouring states is

$$\Delta s^2 = 1 - |\langle r \,|\, r + \mathrm{d}r\rangle|^2 = G_{ij}(r)\,\mathrm{d}x_i \mathrm{d}x_j \quad \big(r = \{x_i\} = \{x, y, z, \cdots\}\big)\,. \quad (1.1)$$

A physical example of G is its appearance in the electric gauge force, beyond Born–Oppenheimer, on a slow system coupled to a fast one [8–10].

[3] Author to whom any correspondence should be addressed.

Here we study the typical behaviour of G_{ij}, by calculating the probability distribution $P_G(G)$ of its trace $G = G_{ii}$. We will emphasise the asymptotic behaviour near the singularities at $G = \infty$, where the distance between states is infinitely sensitive to the parameters, and $G = 0$, where the distance between states is insensitive to the parameters. The statistics discussed here correspond to continuously parameterised families of eigenstates of $N \times N$ matrices drawn from the Gaussian orthogonal ensemble (GOE), where we consider two parameters (x, y), and the Gaussian unitary ensemble (GUE), where we consider three (x, y, z).

The paper is organised as follows. In section 2, we specify the random-matrix models of parameterised Hamiltonians for which we will calculate $P_G(G)$. For consistent comparison between different cases, in particular different N, we will scale the metric trace by $G = gf(N)$, in which $f(N)$ depends on the underlying symmetry, and calculate the scaled distribution $P_g(g)$; the scaling is explained in section 2. We will illustrate the behaviour of $G(\boldsymbol{r})$ for typical members of the ensembles, and, for the GUE, compare this with the related geometric phase curvature [11, 12], whose statistics we have recently explored [13, 14]. In section 3 we employ codimension arguments to anticipate the limiting behaviour of $P_{\mathrm{G}}(G)$ for large and small G. The heart of the paper is sections 4 and 5. Section 4 gives the detailed calculations of $P_G(G)$ and $P_g(g)$ for the GOE, including the N dependence; for $N > 2$ this involves some approximations, so we also compare the theoretical distibutions with numerical simulations. Section 5 describes the corresponding calculations and simulations for the GUE. The appendices A (GOE) and B (GUE) derive the detailed asymptotics of $P_g(g)$ for large and small g.

Throughout the paper we will indicate the $\boldsymbol{r}$ dependence explicitly only where necessary for clarity.

First, some preliminaries. The metric we will study corresponds to the eigenstates $|n(r)\rangle$of a parameterised $N \times N$ Hamiltonian matrix:

$$H(r)\,|n(r)\rangle = E_n(r)\,|n(r)\rangle, \quad (1 \leqslant n \leqslant N)\,. \tag{1.2}$$

$G_{ij}(\boldsymbol{r})$ is the symmetric part of the quantum geometric tensor T_{ij} [9]. For the state $|n(r)\rangle$, this is

$$\begin{aligned} T_{ij}(r) &= \langle \partial_i n|\left(1 - |n\rangle\langle n|\right)|\partial_j n\rangle = \sum_{m\neq n=1}^{N} \langle \partial_i n \mid m\rangle\langle m \mid \partial_j n\rangle \\ &= G_{ij}(r) + \mathrm{i}C_{ij}(r)\,, \quad G_{ij} = G_{ji},\ C_{ij} = -C_{ji}. \end{aligned} \tag{1.3}$$

(Here and hereafter, the index n is implied unless stated otherwise, and $\sum_{m\neq n=1}^{\infty}\cdots$ denotes the double sum $\sum_{m=1}^{\infty}\sum_{n=1,m\neq n}^{\infty}\cdots$). The antisymmetric part C_{ij} is the geometric phase curvature, whose flux through a circuit determines the geometric phase [11], and which also corresponds to the post-Born–Oppenheimer gauge force of geometric magnetism acting on a slow system coupled to a fast one [9,15,16].

Differentiating the eigenequation (1.2) leads to an expression for the metric trace in terms of the matrix elements of ∇H and the energy separations S_{nm}:

$$\begin{aligned} G(r) = \operatorname{tr} G_{ij} &= \sum_{m\neq n=1}^{N} |\langle \nabla n \mid m\rangle|^2 = \sum_{m\neq n=1}^{N} \frac{|\langle n|\,\nabla H\,|m\rangle|^2}{S_{nm}^2}, \\ S_{nm} &= E_n - E_m. \end{aligned} \tag{1.4}$$

The sum of squares in the numerator, and the square in the denominator, reflect the fact that G_{ij} is a positive (semi)definite matrix (i.e. $a_i G_{ij} a_j \geqslant 0$ for any vector a_j). The sum of squares will lead to a characteristic N dependence of $P_G(G)$ for small G, different for the GOE and GUE.

The corresponding geometric phase curvature quantity is the length of the vector represented by the components of the antisymmetric tensor C_{ij}:

$$C(r) = |\mathbf{C}(r)| = |\mathrm{Im}\,\langle\nabla n| \times |\nabla n\rangle| = \left|\mathrm{Im}\sum_{m\neq n=1}^{N} \frac{\langle n|\nabla H|m\rangle \times \langle m|\nabla H|n\rangle}{S_{nm}^2}\right|. \tag{1.5}$$

This vanishes when H is a real symmetric matrix—e.g. for GOE systems, where there is time-reversal symmetry. The curvature does not vanish for GUE systems, but its small C behaviour [13,14] is very different from what we will find for G.

2. Random-matrix models

The statistics of G depend on the number of parameters $\boldsymbol{r}$ in the families of Hamiltonians, but the principles underlying the calculations do not. For definiteness, and bearing in mind the energy denominators in the sum (1.4), we choose the number of parameters as the codimension of degeneracies in the parameter space: two for real symmetric Hamiltonians and three for complex Hermitian Hamiltonians [17]. For simplicity of presentation, we choose families in which the parameter dependence is linear.

Thus, for real symmetric Hamiltonians, the ensemble of families we consider, and the corresponding $G(\boldsymbol{r})$, are

$$\begin{gathered}\mathrm{GOE}: r = \{x, y\}, \quad H(r) = H_0 + xH_1 + yH_2, \\ G(r) = \sum_{m\neq n=1}^{N} \frac{H_{1,nm}^2 + H_{2,nm}^2}{S_{nm}^2}, \quad H_{1,2,nm} = \langle n|H_{1,2}|m\rangle,\end{gathered} \tag{2.1}$$

involving three $N \times N$ matrices H_0, H_1, H_2 drawn independently from the GOE. All matrix elements are real, so the curvature $C(\boldsymbol{r}) = 0$.

For complex Hermitian Hamiltonians, the corresponding ensemble of families, introduced in [18], is

$$\begin{gathered}\mathrm{GUE}: r = \{x, y, z\}, \quad H(r) = H_0 + xH_1 + yH_2 + zH_3, \\ G(r) = \sum_{m\neq n=1}^{N} \frac{|H_{1,nm}|^2 + |H_{2,nm}|^2 + |H_{3,nm}|^2}{S_{nm}^2},\end{gathered} \tag{2.2}$$

involving four $N \times N$ matrices H_0, H_1, H_2, H_3 drawn independently from the GUE. The matrix elements are now complex, so the geometric phase curvature is not zero:

$$\mathrm{GUE}: C(r) = \sqrt{C_x^2 + C_y^2 + C_z^2}, \quad C_x = 2\ \mathrm{Im}\sum_{m\neq n=1}^{N} \frac{H_{2,mn}H_{3,mn}}{S_{mn}^2}, \text{etc.} \tag{2.3}$$

We will denote ensemble averages by $\langle\cdots\rangle$; the similar bra-ket notation for quantum expectation values should not cause confusion.

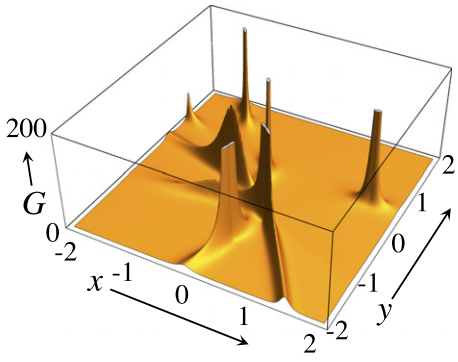

Figure 1. (a) Landscape of the trace $G(\boldsymbol{r})$ as a function of x and y for a GOE family of Hamiltonians, for the state 3 of a 6×6 Hamiltonian. The five infinite spikes correspond to degeneracies: three with the state 2 and two with the state 4 (the large maximum near $x = -1$, $y = +1$ is not a degeneracy).

To scale the metric traces, it would seem natural to use the ensemble mean value $\langle G \rangle$. But, as we will see in section 3, this is infinite for the GOE (as a consequence of level repulsion, itself a consequence of the codimension of degeneracies). However, the fractional moments $\langle G^s \rangle$ $(0 < s < 1)$ are finite, and we choose $s = 1/2$, i.e. the mean $\langle \sqrt{G} \rangle$, with the scaling.

$$\text{GOE}: g = \frac{G}{\langle \sqrt{G} \rangle^2}, \quad P_g(g) = \left\langle \sqrt{G} \right\rangle^2 P_G\left(\left\langle \sqrt{G} \right\rangle^2 g \right). \tag{2.4}$$

This stratagem is not needed for the GUE, because $\langle G \rangle$ is finite, so the corresponding scaling is obvious:

$$\text{GUE}: g = \frac{G}{\langle G \rangle}, \quad P_g(g) = \langle G \rangle P_G\left(\langle G \rangle g \right). \tag{2.5}$$

For all cases, we also calculate the cumulative metric trace distribution:

$$Q_g(g) = \int_0^g \mathrm{d}g' P_g\left(g'\right). \tag{2.6}$$

This is convenient for comparing theory with numerical simulation, because it does not require collecting the data into bins.

It is helpful to illustrate the systems we are studying by displaying an individual family from each of the two ensembles. Figure 1 shows $G(x, y)$ for a GOE family. The infinite spikes correspond to degeneracies: zeros of the denominator $m = n \pm 1$ in (2.1), which have codimension two.

Figure 2(a) shows the analogous $G(x, y, z_0)$ for a GUE family, that is, as a function of x and y for a fixed value z_0. In contrary to the GOE case, there are no infinite spikes, because degeneracies have codimension 3 so they typically do not occur with only two parameters. But we expect, and have found numerically, that there are degeneracies for z values close to z_0, and these zeros of the denominators in (2.2) are responsible for the peaks in figure 2(a): ghosts of nearby degeneracies.

Figure 2(b) shows the geometric phase curvature (2.3) for the same family (i.e. the same four GUE matrices in (2.2)). It looks very similar to figure 2(a), because $C(\boldsymbol{r})$ contains

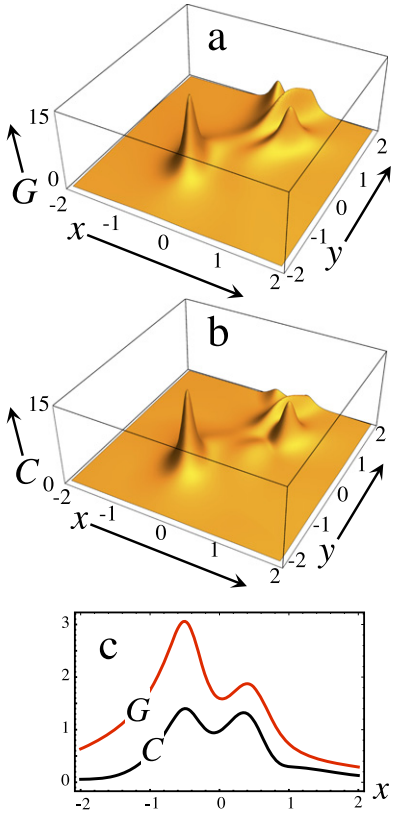

Figure 2. (a) Landscape of the trace $G(\boldsymbol{r})$ for the state 3 in a GUE family of 6×6 Hamiltonians, as a function of x and y for a fixed value of z, showing a maximum associated with a (codimension 3) degeneracy at a nearby value of z. (b) As (a), for the length $C(\boldsymbol{r})$ of the geometric phase curvature vector. (c) Section of (a) and (b) for $y = 0$, showing that the small values of G are much larger than those of C.

the same denominators. But as the sectional graph in figure 2(c) illustrates, the two functions are significantly different; in particular, the small values of G are much larger than those of C, for a fundamental reason, to be explained in the next section (below equation (3.4)).

Although the parameters $\boldsymbol{r}$ do not appear explicitly in the expressions (2.1) and (2.2), they are hidden in the eigenstates $|n\rangle$, $|m\rangle$, and the eigenvalues E_n, E_m, because these constitute the spectrum of the total Hamiltonians H in (2.1) and (2.2), which depends on $\boldsymbol{r}$. But in calculating the statistics we will henceforth set $\boldsymbol{r} = 0$, and then the eigenstates and eigenvalues are those of H_0. This is an important simplification. If we were to reinstate the parameters, this would affect the scaling of the probability distributions but not their form, as was discussed for the geometric phase curvature [13].

3. Codimensions and scaling

Parameter values for which $G = \infty$ or $G = 0$ correspond to singularities of the metric tensor. When $G = \infty$, the quantum state is infinitely sensitive to changes in the parameters, and

when $G = 0$ the state is locally insensitive to such changes. The two singularities give rise to characteristic asymptotic behaviour of $P_G(G)$, different for the GOE and the GUE. Near the different singularities, we will estimate $P_G(G)$ by choosing local parameter-space coordinates whose number equals the codimension. The resulting behaviour will provide a check on the explicit calculations in sections 4 and 5.

3.1. Large G

In (1.4) or (2.1), $G = \infty$ corresponds to zeros of $S_{n,n\pm1}$, i.e. degeneracies. For the GOE, degeneracies have codimension 2, and G diverges quadratically. Therefore we can choose local coordinates ξ_1, ξ_2, and estimate $P_G(G)$ as follows:

$$\mathrm{GOE}: P_G(G) \sim \int \mathrm{d}\xi_1 \int \mathrm{d}\xi_2 \delta\left(G - \frac{1}{\xi_1^2+\xi_2^2}\right) \sim \int \mathrm{d}\rho\rho\delta\left(G - \frac{1}{\rho^2}\right) \sim \frac{1}{G^2}. \tag{3.1}$$

It follows that, as claimed, the mean value of G is infinite but the mean value of $\sqrt{G}$ is finite, justifying the scaling (2.4). For the GUE, degeneracies have codimension 3, and the analogous calculation based on (2.2) gives the estimate

$$\begin{aligned}\mathrm{GUE}: P_G(G) &\sim \int \mathrm{d}\xi_1 \int \mathrm{d}\xi_2 \int \mathrm{d}\xi_3 \delta\left(G - \frac{1}{\xi_1^2+\xi_2^2+\xi_3^2}\right) \\ &\sim \int \mathrm{d}\rho\rho^2\delta\left(G - \frac{1}{\rho^2}\right) \sim \frac{1}{G^{5/2}}.\end{aligned} \tag{3.2}$$

Thus the mean value of G is finite, justifying the scaling (2.5). The power-law (3.2) is the same as for the geometric phase curvature C [13]; for the GOE there is no such analogy because $C = 0$.

3.2. Small G

All matrix elements in (1.4) contribute positively so they must all vanish in order for G to vanish. For the GOE, each of the $N-1$ terms in the sum in (2.1) contains two positive contributions, from x and y, so the codimension of zeros of G is $2(N-1)$. At each such zero, G vanishes quadratically, so

$$\begin{aligned}\mathrm{GOE}: P_G(G) &\sim \int \mathrm{d}\xi_1 \cdots \int \mathrm{d}\xi_{2(N-1)} \delta\left(G - \sum_{i=1}^{2(N-1)} \xi_i^2\right) \\ &\sim \int \mathrm{d}\rho\rho^{2N-3}\delta\left(G-\rho^2\right) \sim G^{N-2}.\end{aligned} \tag{3.3}$$

For the GUE, each of the $N-1$ terms contains six contributions: two from each of x, y and z, from the real and imaginary parts of the complex matrix elements. Therefore the codimension of zeros is $6(N-1)$, and the analogous argument gives

$$\begin{aligned}\mathrm{GUE}: P_G(G) &\sim \int \mathrm{d}\xi_1 \cdots \int \mathrm{d}\xi_{6(N-1)} \delta\left(G - \sum_{i=1}^{6(N-1)} \xi_i^2\right) \\ &\sim \int \mathrm{d}\rho\rho^{6N-7}\delta\left(G-\rho^2\right) \sim G^{3N-4}.\end{aligned} \tag{3.4}$$

Both N dependences for small G are consequences of the sums of squares in the numerators for the formulas (2.1) and (2.2); this behaviour of the metric trace is very different from the curvature C, whose corresponding numerator in (2.3) does not involve sums of squares. The expressions (3.3) and (3.4) indicate that in the limit of infinite matrices $P_G(G)$ must vanish faster than any power of G, i.e. $G = 0$ is an essential singularity, whose explicit forms for GOE and GUE we derive in appendices A and B.

4. GOE calculations

From (2.1), and the representation of a probability distribution as the average of a δ-function, we have

$$\begin{aligned} P_G(G) &= \left\langle \delta\left(G - \sum_{m\neq n=1}^{N} \frac{H_{1,nm}^2 + H_{2,nm}^2}{S_{nm}^2}\right)\right\rangle \\ &= \frac{1}{2\pi}\int_{-\infty}^{\infty} \mathrm{d}t\, \exp(-\mathrm{i}Gt)\left\langle \prod_{m\neq n=1}^{N} \exp\left(\mathrm{i}t\frac{\left(H_{1,nm}^2 + H_{2,nm}^2\right)}{S_{nm}^2}\right)\right\rangle. \end{aligned} \tag{4.1}$$

The ensemble average is over the GOE matrix elements and eigenvalue separations; these are statistically independent; moreover, in $H_{1,nm}$ and $H_{2,nm}$ the GOE matrices are independent of the eigenstates n and m of H_0. Therefore the averages can be evaluated separately, starting with the matrix elements. These are real and Gauss-distributed, and we can normalise them arbitrarily because we will scale $P_G(G)$ according to (2.4). Thus we take

$$\left\langle H_{nm}^2\right\rangle = \frac{1}{2} \Rightarrow P_H(H_{nm}) = \frac{1}{\sqrt{\pi}}\exp\left(-H_{nm}^2\right). \tag{4.2}$$

The average over matrix elements in (4.1) is

$$\left\langle \prod_{m\neq n=1}^{N} \exp\left(\mathrm{i}t\frac{\left(H_{1,nm}^2 + H_{2,nm}^2\right)}{S_{nm}^2}\right)\right\rangle = \left\langle \prod_{m\neq n=1}^{N} \frac{1}{1-\mathrm{i}t/S_{nm}^2}\right\rangle_{S_{nm}}. \tag{4.3}$$

4.1. GOE theory, N=2

There are only two eigenvalues, so the product in (4.3) has only one factor, involving the spacing $S = S_2 - S_1$, whose distribution, with the mean value of S chosen as unity, has the well known Wigner form [19]

$$P_S(S) = \frac{\pi S}{2}\exp\left(-\frac{\pi S^2}{4}\right), \tag{4.4}$$

Thus the metric trace distribution can be evaluated by integrating over t first and then averaging over S:

$$P_G(G) = \frac{\mathrm{i}S^2}{2\pi}\left\langle \int_{-\infty}^{\infty}\mathrm{d}t\frac{\exp(-\mathrm{i}Gt)}{t+\mathrm{i}S^2}\right\rangle_S = \left\langle S^2\exp\left(-S^2G\right)\right\rangle_S = \frac{4\pi}{(4G+\pi)^2}. \tag{4.5}$$

This agrees with the limits in (3.1) and (3.3).

The average required for scaling is

$$\left\langle \sqrt{G} \right\rangle = \frac{\pi^{3/2}}{4} = 1.3921, \tag{4.6}$$

so the scaled distribution, with $\left\langle \sqrt{g} \right\rangle = 1$, is

$$P_g(g) = \frac{4}{\pi^2 \left(g + 4/\pi^2\right)^2}. \tag{4.7}$$

This result is exact. The associated cumulative distribution, also exact, is

$$Q_g(g) = \frac{g}{g + 4/\pi^2}. \tag{4.8}$$

4.2. GOE theory, N=3

Now there are three states 1, 2, 3, and we calculate $P_G(G)$ for the state 2, so there are two spacings. Thus the distribution involving the required average (4.3), is

$$P_G(G) = \frac{1}{2\pi} \left\langle \int_{-\infty}^{\infty} \mathrm{d}t \frac{\exp(-\mathrm{i}Gt)}{\left(1 - \mathrm{i}t/S_1^2\right)\left(1 - \mathrm{i}t/S_2^2\right)} \right\rangle_{S_1,S_2}. \tag{4.9}$$

Evaluating the t integral gives

$$P_G(G) = \left\langle \frac{S_1^2 S_2^2 \left(\exp\left(-S_1^2 G\right) - \exp\left(-S_2^2 G\right)\right)}{S_2^2 - S_1^2} \right\rangle_{S_1,S_2}. \tag{4.10}$$

The neighbouring spacings S_1 and S_2 are correlated [19], but the correlation is weak ($\langle S_1 S_2 \rangle / \langle S_1 \rangle^2 - 1 \approx -0.069$), and, as in our geometric curvature theory [13], we neglect it. For these spacings, we use the Wigner distribution (4.4), which is a close approximation for the $N = 3$ eigenvalue spacings [19]. The integrals over S_1 and S_2 can be evaluated explicitly, with the result

$$P_G(G) = \frac{8\pi G}{(2G + \pi)^2 (4G + \pi)} + \frac{2\pi^2 \log\left(1 + 4G/\pi\right)}{(2G + \pi)^3}, \tag{4.11}$$

again agreeing with the limits (3.1) and (3.3). The required average is

$$\left\langle \sqrt{G} \right\rangle = \sqrt{\frac{\pi^3}{2^5}} \left(\sqrt{2} + \coth^{-1}\sqrt{2}\right) = 2.259\,66, \tag{4.12}$$

from which the scaled $P_g(g)$, with $\left\langle \sqrt{g} \right\rangle = 1$, follows from (2.4). The cumulative distribution (2.6) is

$$Q_g(g) = \left(1 - \frac{\pi\left(4G + \pi\left(2 - \log\,\pi\right) + \pi\,\log\left(4G + \pi\right)\right)}{2(2G + \pi)^2}\right)_{G = \left\langle \sqrt{G} \right\rangle^2 g} \tag{4.13}$$

4.3. GOE theory, $N \to \infty$

Now there are infinitely many eigenvalue separations. For the two closest, $m = n \pm 1$, we again use the uncorrelated Wigner distibutions (4.4). For the non-nearest-neighbour separations $m = n \pm k$, $k \geqslant 2$, the rigidity of the spectrum suggests approximating the separations by their mean values:

$$S_{n,n\pm k} \approx \pm k, \quad (k \geqslant 2)\,, \tag{4.14}$$

in which we have incorporated the mean eigenvalue spacing unity. Although this approximation exaggerates the correlations between distant eigenvalues, it agrees well with numerics for large N; we could incorporate the known distant-level correlation [19], but then subsequent integrations would be intractable.

Thus the metric trace distribution is

$$P_G\,(G) = \frac{1}{2\pi}\int_{-\infty}^{\infty} \mathrm{d}t\, \exp\left(-\mathrm{i}Gt\right) \left\langle \frac{1}{\left(1-\mathrm{i}t/S^2\right)} \right\rangle_S^2 \prod_{k=2}^{\infty} \frac{1}{\left(1-\mathrm{i}t/k^2\right)^2}. \tag{4.15}$$

The infinite product can be evaluated exactly:

$$\prod_{k=2}^{\infty} \frac{1}{\left(1-\mathrm{i}t/k^2\right)^2} = -\frac{\mathrm{i}\pi^2 t(\mathrm{i}+t)^2}{\sin^2\left(\pi\sqrt{\mathrm{i}t}\right)} \equiv h\,(t)\,. \tag{4.16}$$

The integral over t could be evaluated in terms of the residues at the infinite string of poles at $t = -\mathrm{i}S^2$ and $t = -\mathrm{i}k^2$, but the resulting expressions are cumbersome, and the subsequent integrations over the separations intractable. Therefore we evaluate the two S averages first, using

$$\begin{gathered} \left\langle \frac{1}{\left(1-\mathrm{i}t/S^2\right)} \right\rangle_S^2 = f\,(t) = f_0\,(t)\,\Theta\,(t) + f_0^*\,(-t)\,\Theta\,(-t)\,, \\ \text{where } f_0\,(t) = \left(1 - \frac{1}{4}\pi t\, \exp\left(-\frac{1}{4}\mathrm{i}\pi t\right)\left(\pi + \mathrm{i}E\mathrm{i}\left(\frac{1}{4}\mathrm{i}\pi t\right)\right)\right)^2. \end{gathered} \tag{4.17}$$

Thus (4.15) can be written in terms of a single integral:

$$P_g\,(g) = \frac{\left\langle\sqrt{G}\right\rangle^2}{2\pi}\int_{-\infty}^{\infty} \mathrm{d}t\, \exp\left(-\mathrm{i}\left\langle\sqrt{G}\right\rangle^2 gt\right) h\,(t)\, f\,(t)\,. \tag{4.18}$$

It does not seem possible to evaluate this in closed form, but it can be computed numerically. For the average required for scaling, it is more efficient to integrate over G first, leaving the following limit of the integral over t:

$$\left\langle\sqrt{G}\right\rangle = \frac{1}{2\pi}\lim_{G\to\infty}\int_{-\infty}^{\infty} \mathrm{d}t \frac{\left(2\mathrm{i}t\sqrt{G}\, \exp\left(-\mathrm{i}Gt\right) - \sqrt{\pi\mathrm{i}t}\,\mathrm{erf}\left(\sqrt{\mathrm{i}Gt}\right)\right) f\,(t)\, h\,(t)}{2t^2} \approx 2.64 \tag{4.19}$$

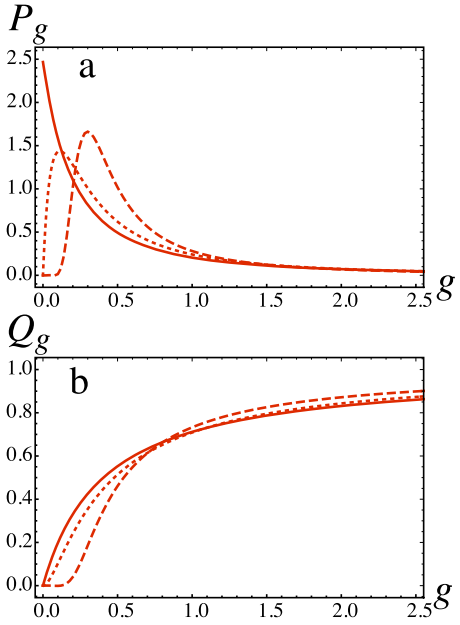

Figure 3. (a) $P_g(g)$ for GOE statistics for $N = 2$ (full curve, equation (4.7)), $N = 3$ (dotted curve, equation (4.11)), $N = \infty$ (dashed curve, equation (4.18)). All three distributions have $\left\langle \sqrt{g} \right\rangle = 1$. (b) as (a), for $Q_g(g)$.

The cumulative distribution is, similarly,

$$Q_g(g) = \frac{1}{2\pi}\int_{-\infty}^{\infty} \mathrm{d}t \left(1 - \exp\left(-\mathrm{i}\left\langle\sqrt{G}\right\rangle^2 gt\right)\right) \frac{h(t)\, f^2(t)}{\mathrm{i}t}. \tag{4.20}$$

The large N asymptotic behaviour of (4.18) for large and small g, derived in appendix A, is

$$P_g(g) \approx \begin{cases} \dfrac{\pi}{2\left\langle\sqrt{G}\right\rangle^2 g^2} = \dfrac{0.2254}{g^2} & (g >> 1) \\ \dfrac{64\pi^{5/2}}{\left\langle\sqrt{G}\right\rangle^5} g^{-7/2} \exp\left(-\dfrac{\pi^2}{\left\langle\sqrt{G}\right\rangle^2 g}\right) \approx 8.730 g^{-7/2} \exp\left(-\dfrac{1.416}{g}\right) & (g << 1) \end{cases} \tag{4.21}$$

These results are consistent with the codimension arguments in section 3.

Figure 3 shows the scaled distributions, and the cumulative distributions, for the GOE, for $N = 2$, $N = 3$ and $N = \infty$.

4.4. GOE numerical simulations

We computed G from (2.1) for 20 000 samples of the three GOE matrices, for several values of N, and the corresponding values of $\left\langle\sqrt{G}\right\rangle$and hence g. $P_g(g)$ can be computed from the

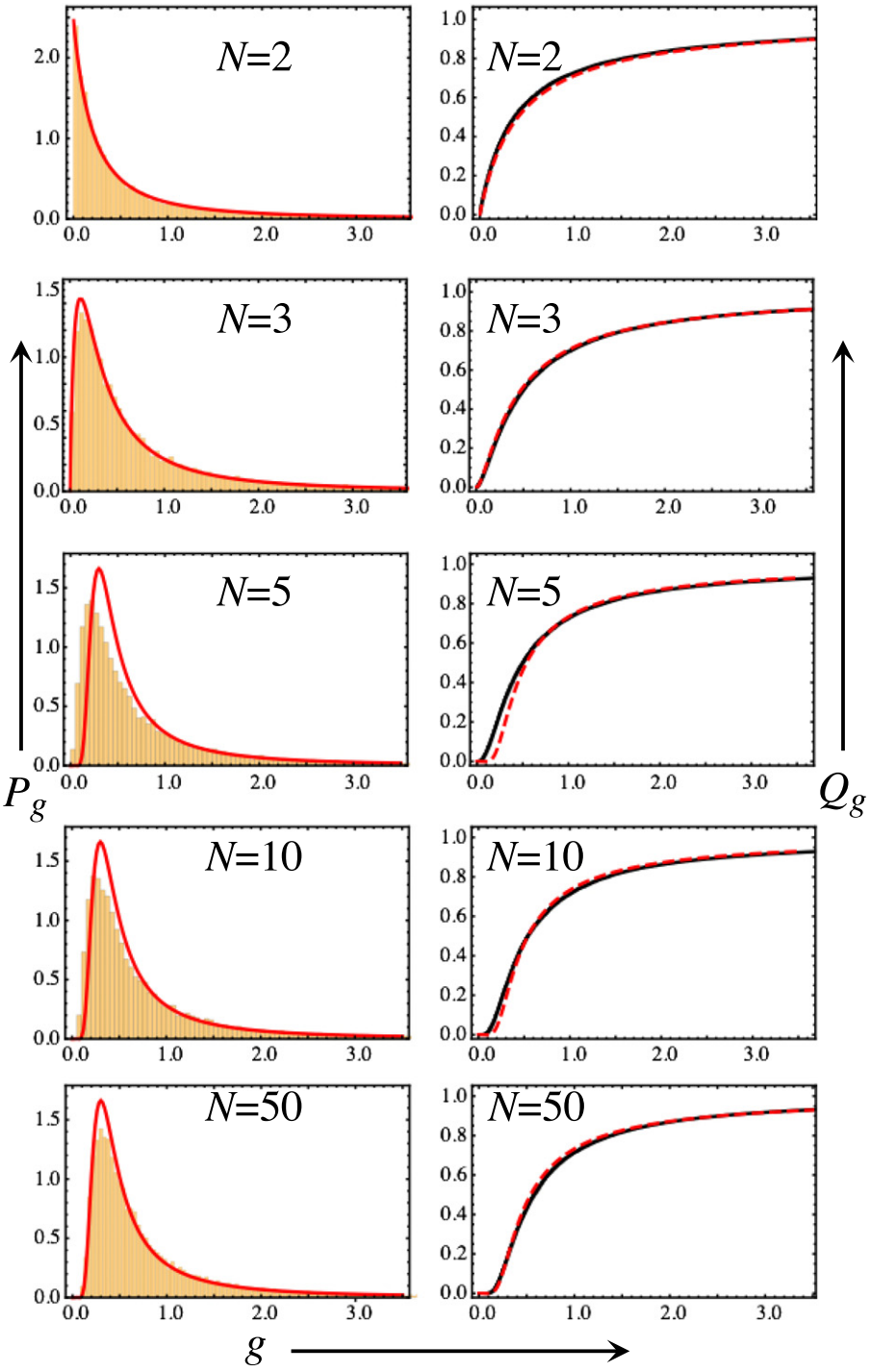

Figure 4. Metric tensor GOE trace distributions $P_g(g)$ (left panels) and cumulative distributions $Q_g(g)$ (right panels), for the indicated values of N. For $P_g(g)$, the simulations are the histograms, and the theory is the full red curves; for $Q_g(g)$, the simulations are the full black curves, and the theory is the dashed red curves.

histogram of values of g. $Q_g(g)$ can be obtained by plotting the ordered list of g values. Figure 4 shows the results. The agreement with theory is excellent. For $N = 2$ this is not surprising, because the formulas (4.7) and (4.8) are exact. The agreement for $N = 3$, and the convergence onto the $N \to \infty$ theory for $N = 5, 10, 50$, justify the approximations for the eigenvalue separations.

5. GUE calculations

For the GUE, the calculations leading to $P_g(g)$ are slightly more complicated than for GOE but the principles are the same. Therefore we state the results and only outline the derivations. Instead of (4.1), and using (2.2), the distribution of the unscaled G is

$$P_G(G) = \left\langle \delta\left(G - \sum_{m\neq n=1}^{N} \frac{|H_{1,nm}|^2 + |H_{2,nm}|^2 + |H_{3,nm}|^2}{S_{nm}^2}\right)\right\rangle$$
$$= \frac{1}{2\pi}\int_{-\infty}^{\infty} \mathrm{d}t\, \exp(-\mathrm{i}Gt)\left\langle \prod_{m\neq,n=1}^{N} \exp\left(\mathrm{i}t\frac{\left(|H_{1,nm}|^2 + |H_{2,nm}|^2 + |H_{3,nm}|^2\right)}{S_{nm}^2}\right)\right\rangle. \tag{5.1}$$

Now the matrix elements are complex, with their real and imaginary parts Gauss-distributed, so we can take, by analogy with (4.2),

$$H_{mn} = a + \mathrm{i}b, \quad \left\langle a^2\right\rangle = \left\langle b^2\right\rangle = \frac{1}{2} \Rightarrow P_a(a) = P_b(a) = \frac{1}{\sqrt{\pi}}\exp\left(-a^2\right). \tag{5.2}$$

For each m in the product, there are now six real matrix elements, so the average over them gives

$$\left\langle \prod_{m\neq n=1}^{N} \exp\left(\mathrm{i}t\frac{\left(|H_{1,nm}|^2 + |H_{2,nm}|^2 + |H_{3,nm}|^2\right)}{S_{nm}^2}\right)\right\rangle = \left\langle \prod_{m\neq n=1}^{N} \frac{1}{\left(1 - \mathrm{i}t/S_{mn}^2\right)^3}\right\rangle_{S_{mn}}. \tag{5.3}$$

5.1. GUE theory, $N = 2$

There is only one separation, namely the spacing, $S = S_2 - S_1$, whose GUE distribution, replacing (4.4), is

$$P_S(S) = \frac{32S^2}{\pi^2}\exp\left(-\frac{4S^2}{\pi}\right). \tag{5.4}$$

Thus

$$P_G(G) = -\frac{\mathrm{i}S^6}{2\pi}\left\langle \int_{-\infty}^{\infty} \mathrm{d}t \frac{\exp(-\mathrm{i}Gt)}{\left(t+\mathrm{i}S^2\right)^3} \right\rangle_S = \frac{1}{2}G^2\left\langle S^6 \exp\left(-S^2G\right)\right\rangle_S$$
$$= \frac{105G^2}{2\pi^{3/2}\left(G+4/\pi\right)^{9/2}}. \tag{5.5}$$

This agrees with the limits in (3.2) and (3.4).

Now the average over G converges, and can be used for scaling:

$$\langle G\rangle = \frac{24}{\pi}, \tag{5.6}$$

so the scaled distribution, with $\langle g\rangle = 1$, is, exactly,

$$P_g(g) = \frac{2835g^2}{2(1+6g)^{9/2}}. \tag{5.7}$$

The associated cumulative distribution is

$$Q_g(g) = 1 - \frac{1+21g+315g^2/2}{(1+6g)^{7/2}}. \tag{5.8}$$

5.2. GUE theory, $N = 3$

Now there are two spacings, and the GUE version of (4.9) is

$$P_G(G) = \frac{1}{2\pi}\left\langle \int_{-\infty}^{\infty} \mathrm{d}t \frac{\exp(-\mathrm{i}Gt)}{\left(1-\mathrm{i}t/S_1^2\right)^3\left(1-\mathrm{i}t/S_2^2\right)^3} \right\rangle_{S_1,S_2}. \tag{5.9}$$

With the notation $a \equiv S_1^2$, $b \equiv S_2^2$, the t integral can be evaluated:

$$P_G(G) = \left\langle a^3b^3\left[\exp(-aG)\left(\frac{6}{(b-a)^5} - \frac{3G}{(b-a)^4} + \frac{G^2}{2(b-a)^3}\right)\right.\right.$$
$$\left.\left. - \exp(-bG)\left(\frac{6}{(b-a)^5} + \frac{3G}{(b-a)^4} + \frac{G^2}{2(b-a)^2}\right)\right]\right\rangle_{S_1,S_2}. \tag{5.10}$$

Again we use the approximation that S_1 and S_2 are uncorrelated $\left(\langle S_1S_2\rangle / \langle S_1\rangle^2 - 1 \approx -0.050\right)$; this leads to

$$P_G(G) = \frac{105\pi^6G^5\left(448+112\pi G+\pi^2G^2\right)}{(4+\pi G)^{3/2}(8+\pi G)^8}, \tag{5.11}$$

again agreeing with (3.2) and (3.4). The required average is

$$\langle G\rangle = \frac{48}{\pi}, \tag{5.12}$$

so the scaled distribution, with $\langle g\rangle = 1$, is

$$P_g(g) = \frac{612\,360g^5\left(7+84g+36g^2\right)}{(1+12g)^{3/2}(1+6g)^8}. \tag{5.13}$$

The associated cumulative distribution is

$$\begin{aligned} Q_g(g) &= \frac{H(g,F(g))}{(1+6g)^7 F(g)}, \quad \text{where } F(g) = \sqrt{1+12g}, \\ H(g,F) &= F - 1 + g(42F-48) + g^2(756F-990) + g^3(7560F-11\,448) \\ &\quad + g^4(45\,360F-80\,838) + g^5(163\,296F-353\,808) \\ &\quad + g^6(326\,592F-204\,120) + 279\,936g^7. \end{aligned} \tag{5.14}$$

5.3. GUE theory, $N \to \infty$

Again using the approximation (4.14) that the non-nearest-neighbour separations can be replaced by their means, we obtain the GUE counterpart of (4.15):

$$P_G(G) = \frac{1}{2\pi}\int_{-\infty}^{\infty} \mathrm{d}t\, \exp(-\mathrm{i}Gt) \left\langle \frac{1}{\left(1-\mathrm{i}t/S^2\right)^3} \right\rangle_S^2 \prod_{k=2}^{\infty} \frac{1}{\left(1-\mathrm{i}t/k^2\right)^6}. \tag{5.15}$$

The product is the cube of $h(t)$ in (4.16). The average over the two nearest spacings is

$$\begin{aligned} \left\langle \frac{1}{\left(1-\mathrm{i}t/S^2\right)^3} \right\rangle_S^2 &= \left(\frac{32\mathrm{i}}{\pi^2}\int_0^{\infty} \mathrm{d}S \frac{S^8}{\left(t+\mathrm{i}S^2\right)} \exp\left(-\frac{4S^2}{\pi}\right)\right)^2 \equiv f_1(t), \quad \text{where} \\ f_1(t) &= \left(\frac{2}{\pi^3\sqrt{\mathrm{i}}} \exp\left(-\frac{4\mathrm{i}t}{\pi}\right) t^{3/2}\left(35\pi^2 - 112\mathrm{i}\pi t - 64t^2\right)\left(\mathrm{erfi}\left(2\sqrt{\frac{\mathrm{i}t}{\pi}}\right) - \mathrm{i}\right)\right. \\ &\quad \left. + \frac{1}{\pi^3}\left(\pi^3 + 24\mathrm{i}\pi^2 t + 104\pi t^2 - 64\mathrm{i}t^3\right)\right)^2. \end{aligned} \tag{5.16}$$

Thus the GUE metric trace distribution, the counterpart of (4.18), is

$$P_g(g) = \frac{\langle G\rangle}{2\pi}\int_{-\infty}^{\infty} \mathrm{d}t\, \exp\left(-\mathrm{i}\langle G\rangle gt\right) h^3(t)\, f_1(t). \tag{5.17}$$

As with the GOE distribution, this integral can be evaluated numerically. The average required for scaling is

$$\langle G\rangle = \frac{1}{2\pi}\lim_{G\to\infty}\int_{-\infty}^{\infty} \mathrm{d}t \frac{(\exp(-\mathrm{i}Gt)(1+\mathrm{i}Gt)-1)\, t(t+\mathrm{i})^6}{t^2} h^3(t)\, f_1(t) \approx 19.25 \tag{5.18}$$

The cumulative distribution is

$$Q_g(g) = \frac{1}{2\pi\mathrm{i}}\int_{-\infty}^{\infty} \mathrm{d}t \frac{\left(1-\exp\left(-\mathrm{i}\langle G\rangle gt\right)\right)}{t} h^3(t)\, f_1(t). \tag{5.19}$$

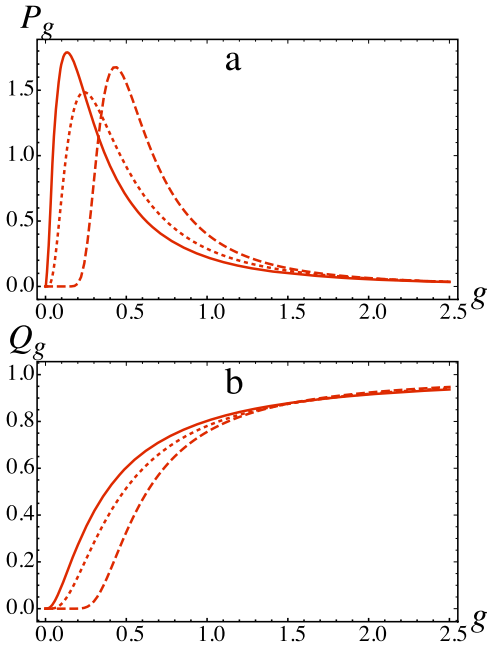

Figure 5. (a) $P_g(g)$ for a family of GUE Hamltonians. $N = 2$ (full curve, equation (5.7)), $N = 3$ (dotted curve, equation (5.13)), $N = \infty$ (dashed curve, equation (5.17)). All three distributions have $\langle g \rangle = 1$. (b) as (a), for $Q_g(g)$.

The large N asymptotic behaviour of (5.17) for large and small g, derived in appendix B, is

$$P_g(g) \approx \begin{cases} \dfrac{105}{\left(\pi \langle G \rangle\right)^{3/2} g^{5/2}} = \dfrac{0.223}{g^{5/2}} \quad (g >> 1) \\ \dfrac{\pi^{37/2} 24\,111\,675}{4096 \langle G \rangle^{13/2}} g^{-15/2} \exp\left(-\dfrac{9\pi^2}{\langle G \rangle g}\right) \\ \approx 41\,556.0 g^{-15/2} \exp\left(-\dfrac{4.615}{g}\right) (g << 1) \end{cases} \tag{5.20}$$

These results are consistent with the codimension arguments in section 3.

Figure 5 shows the theoretical GUE distributions for $N = 2$, $N = 3$ and $N = \infty$—the counterpart of the GOE distributions in figure 3.

5.4. GUE numerical simulations

We computed G from (2.2) for 20 000 samples of the four GUE matrices, for several values of N, and the corresponding values of $\langle G \rangle$ and hence g. Again $P_g(g)$ can be computed from the histogram of values of g, and $Q_g(g)$ by plotting the ordered list of g values. Figure 6 shows the results—the counterpart of figure 4 for the GOE. Again the agreement with theory is excellent. For $N = 2$ this is not surprising, because the formulas (4.7) and (5.8) are exact. The agreement for $N = 3$, and the convergence onto the $N \to \infty$ theory for $N = 5$, 10, 50, justify the approximations for the eigenvalue separations.

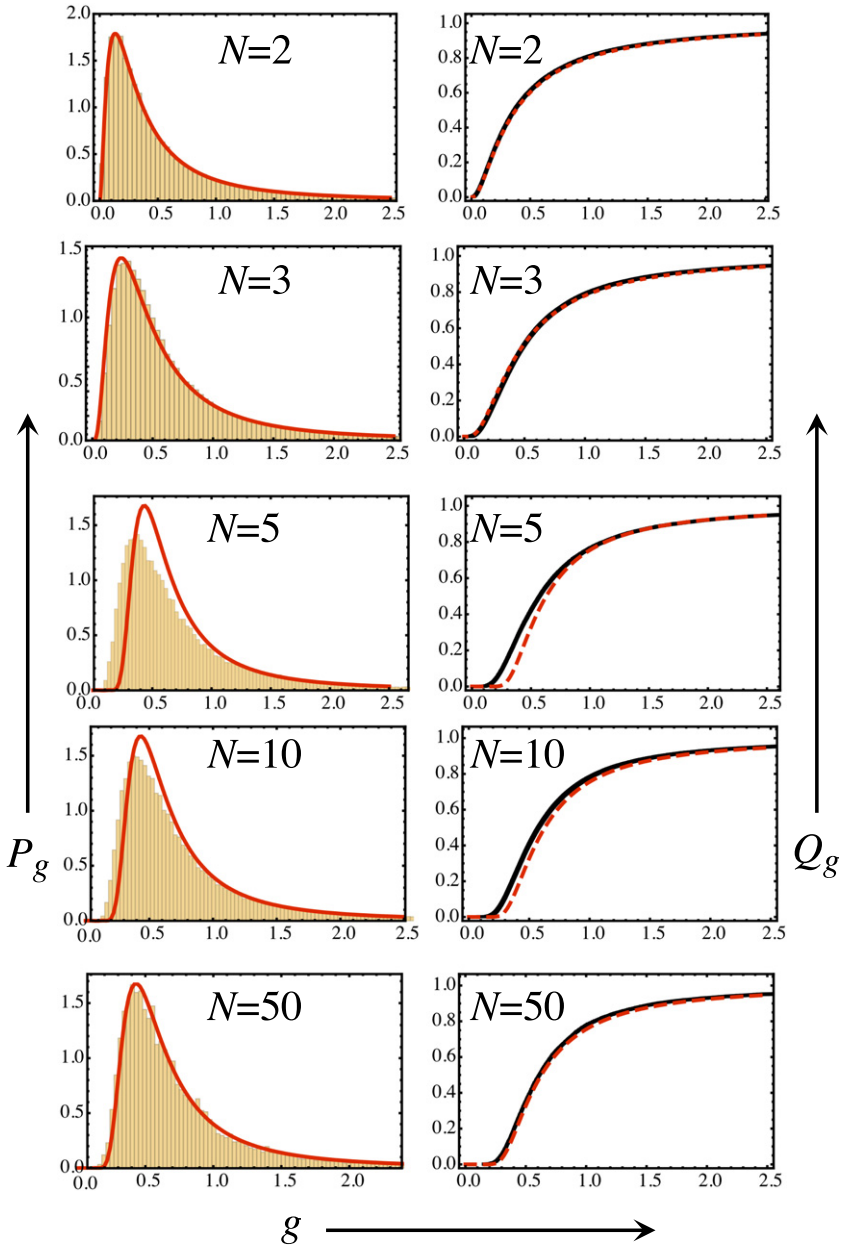

Figure 6. Metric tensor GUE trace distributions $P_g(g)$ (left panels) and cumulative distributions $Q_g(g)$ (right panels), for the indicated values of N. For $P_g(g)$, the simulations are the histograms, and the theory is the full red curves; for $Q_g(g)$, the simulations are the full black curves, and the theory is the dashed red curves.

6. Concluding remarks

The main results of our study are formulas for the scaled probability distributions $P_g(g)$ of the quantum metric tensor trace G, for eigenstates of $N \times N$ matrices depending on

two parameters (GOE, section 4) and three parameters (GUE, section 5), choices reflecting the codimensions of eigenvalue degeneracies. These are fat-tailed distribution; for the GOE, the mean $\langle G\rangle$ is infinite, but $\langle\sqrt{G}\rangle$ is finite, leading to the scale-independent trace $g = G/\langle\sqrt{G}\rangle^2$; for the GUE, the variance $\langle G^2\rangle$ is infinite, but $\langle G\rangle$ is finite, so the scaled trace is$g = G/\langle G\rangle$. Codimension arguments in section 3 established the scaling behaviour of $P_g(g)$ near the singularities at $G = \infty$ and $G = 0$, with explicit coefficients derived in appendix A (GOE) and appendix B (GUE).

These results do not exhaust the statistics of the quantum metric tensor. Many extensions can be envisaged. For the explicit random-matrix models considered, these include

- the distribution of the invariant det$G$;
- the distributions of the three eigenvalues of the tensor G_{ij}.

More elaborate random-matrix models could include

- different numbers of parameters, beyond our two (GOE) and three (GUE);
- combinations of GOE and GUE matrices in the same ensemble, e.g. sparse or structured ensembles representing localised or multifractal eigenstates;
- ensembles where the matrix elements are correlated;
- calculations of statistics of the Riemannian curvature tensor in parameter space, associated with the quantum metric (different from the geometric phase curvature in (1.3) and (1.5)); this depends on derivatives of G_{ij}, and could be calculated for parameters $\boldsymbol{r} \neq 0$, or families depending nonlinearly on the parameters.

Appendix A. GOE metric tensor trace asymptotics for large and small *G*

(i). *GOE* $N \to \infty$, *large* g

For large G or g, the integral (4.18) is dominated by the behaviour of the nonexponential factor in the integrand for small t. Using (4.17), this is

$$h(t)\, f^2(t) = a_0 + a_1 t + \frac{1}{2}\mathrm{i}\pi t \,\log\, t + \cdots, \tag{A.1}$$

where a_1 and a_2 are constants.

The first two terms contribute zero to the integral (4.18), because the contour can be shifted to Im $t = -\infty$, where $\exp\left(-\mathrm{i}\,\langle G\rangle\, gt\right)$ vanishes. The large g asymptotics of $P_g(g)$ is determined by the third term, in which the t contour can be deformed to surround the cut on the negative imaginary axis, where $\log t$ contributes its discontinuity $2\pi\mathrm{i}$. Elementary manipulations then give

$$P_g(g) \approx \frac{\pi}{2\langle\sqrt{G}\rangle^2 g^2} = \frac{0.2254}{g^2} \quad (g >> 1)\,. \tag{A.2}$$

Figure 7(a) illustrates the convergence to this limiting form.

(ii). *GOE* $N \gg 1$, *small* g

The asymptotics of (4.17) will depend in the behaviour of the integrand at a saddle-point high in the upper t half-plane, avoiding the simple poles of $1/\sin^2\left(\pi\sqrt{\mathrm{i}t}\right)$ (cf (4.16)), which lie at $t = -\mathrm{i}n^2$ (n integer). In this region $1/\sin^2\left(\pi\sqrt{\mathrm{i}t}\right)$ is dominated by one of its

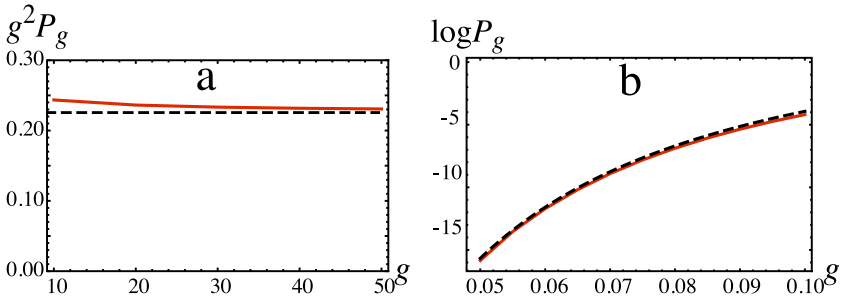

Figure 7. (a) Large g: convergence of $g^2P_g(g)$ (full red curve) for a GOE family of Hamiltonians to the theoretical limit (A.2) (dashed line). (b) Small g: convergence of $\log P_g(g)$ (full red curve) to the theoretical asymptotic formula (A.6) (dashed curve).

two exponentials. We will be interested in Im $t \gg 1$, for which

$$f(t) \approx -\frac{16}{\pi^2 t^2} \quad (\text{Im } t >> 1)\,. \tag{A.3}$$

Thus

$$P_g(g) \approx -\frac{32\left\langle\sqrt{G}\right\rangle^2}{\pi}\mathrm{i}\int_{-\infty}^{\infty}\mathrm{d}t\,t\,\exp\left(-\mathrm{i}\left\langle\sqrt{G}\right\rangle^2 gt + 2\mathrm{i}\pi\sqrt{\mathrm{i}t}\right). \tag{A.4}$$

This integral can be evaluated exactly, but to get the leading-order asymptotics it is simpler to use the steepest-descent approximation [20], based on the saddle-point in the exponent, at

$$t = t_{\text{saddle}} = \frac{\pi^2}{\left(g\left\langle\sqrt{G}\right\rangle\right)^2}\mathrm{i}. \tag{A.5}$$

Straightforward application of this technique determines the essential singularity at $g = 0$:

$$\begin{aligned} P_g(g) &\approx \frac{64\pi^{5/2}}{\left\langle\sqrt{G}\right\rangle^5} g^{-7/2}\,\exp\left(-\frac{\pi^2}{\left\langle\sqrt{G}\right\rangle^2 g}\right) \\ &\approx 8.730 g^{-7/2}\,\exp\left(-\frac{1.416}{g}\right) \quad (g << 1)\,. \end{aligned} \tag{A.6}$$

Figure 7(b) illustrates the convergence to this limiting form.

Appendix B. GUE metric tensor trace asymptotics for large and small *G*

(i). *GUE* $N \to \infty$, *large* g

For large G or g, the integral (5.17) is dominated by the behaviour of the nonexponential factor in the integrand for small t. Using (5.16), this is

$$h^3(t)\,f_1(t) = -1 - \mathrm{i}\frac{\left(48 - 6\pi + \pi^3\right)}{\pi}t + \frac{140\sqrt{\mathrm{i}}}{\pi}t^{3/2} + \cdots \tag{B.1}$$

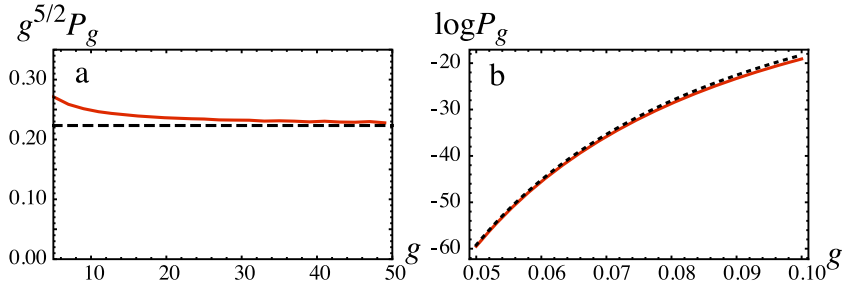

Figure 8. (a) Large g: convergence of $g^{5/2}P_g(g)$ (full red curve) for a GUE family of Hamiltonians to the theoretical limit (B.2) (dashed line). (b) Small g: convergence of $\log P_g(g)$ (full red curve) to the theoretical asymptotic formula (B.6) (dashed curve).

The first two terms contribute zero to the integral (5.17), because the contour can be shifted to $\mathrm{Im}\, t = -\infty$, where $\exp\left(-\mathrm{i}\langle G\rangle gt\right)$ vanishes. The large g asymptotics of $P_g(g)$ is determined by the third term, in which the t contour can be deformed to surround the cut on the negative imaginary axis. Contour integration then gives

$$P_g(g) \approx \frac{105}{\left(\pi\langle G\rangle\right)^{3/2} g^{5/2}} = \frac{0.223}{g^{5/2}} \quad (g >> 1)\,. \tag{B.2}$$

Figure 8(a) illustrates the convergence to this limiting form.

(ii). *GOE $N \gg 1$, small g*

As with the GOE counterpart, the integral (5.17) is dominated by a saddle-point high on the imaginary axis. The relevant limiting behaviour is

$$f_1(t) \approx -\frac{11\,025\pi^6}{262\,144t^6} \quad (\mathrm{Im}\ t >> 1)\,. \tag{B.3}$$

The factor $1/\sin\left(\pi\sqrt{\mathrm{i}t}\right)^6$ is dominated by one of its exponentials, leading to

$$P_g(g) \approx \frac{2^5 11\,025\pi^{11}\langle G\rangle}{262\,144}\int_{-\infty}^{\infty} \mathrm{d}t t^3\, \exp\left(-\mathrm{i}\langle G\rangle gt + 6\mathrm{i}\pi\sqrt{\mathrm{i}t}\right). \tag{B.4}$$

The saddle point of the exponent is at

$$t = t_{\mathrm{saddle}} = \frac{9\pi^2}{\left(g\langle G\rangle\right)^2}\mathrm{i}, \tag{B.5}$$

from which application of steepest-descents gives

$$\begin{aligned} P_g(g) &\approx \frac{\pi^{37/2} 24\,111\,675}{4096\langle G\rangle^{13/2}} g^{-15/2}\, \exp\left(-\frac{9\pi^2}{\langle G\rangle g}\right) \\ &\approx 41\,556.0 g^{-15/2}\, \exp\left(-\frac{4.615}{g}\right) \quad (g << 1)\,. \end{aligned} \tag{B.6}$$

Figure 8(b) illustrates the convergence to this limiting form.

ORCID iDs

M V Berry https://orcid.org/0000-0001-7921-2468
Pragya Shukla https://orcid.org/0000-0001-5308-6520

References

[1] Gianfrate A *et al* 2020 Measurement of the quantum geometric tensor and of the anomalous Hall drift *Nature* **578** 381–6
[2] Piéchon F, Raoux A, Fuchs J-N and Montambaux G 2016 Geometrical orbital susceptibility: quantum metric without Berry curvature *Phys. Rev.* B **94** 134423
[3] Liang L, Peotta S, Harju A and Törma P 2017 Wave-packet dynamics of Bogoliubov quasiparticles: quantum metric effects *Phys. Rev.* B **96** 064511
[4] Zanardi P, Giorda P and Cozzini M 2007 Information-theoretic differential geometry of quantum phase transitions *Phys. Rev. Lett.* **99** 100603
[5] Kolodrubetz M, Gritsev V and Polkovnikov A 2013 Classifying and measuring the geometry of the quantum ground state manifold *Phys. Rev.* B **88** 064304
[6] Werner M A, Brataas A, von Oppen F and Zaránd G 2019 Universal scaling theory of the boundary geometric tensor in disordered metals *Phys. Rev. Lett.* **122** 106601
[7] Provost J P and Vallee G 1980 Riemannian structure on manifolds of quantum states *Commun. Math. Phys.* **76** 289–301
[8] Zygelman B 1987 Appearance of gauge potentials in atomic collision physics *Phys. Lett.* A **125** 476–81
[9] Berry M V 1989 *The Quantum Phase* (*Five Years After in Geometric Phases in Physics*) ed A Shapere and F Wilczek (Singapore: World Scientific) pp 7–28
[10] Berry M V and Lim R 1990 The Born–Oppenheimer electric gauge force is repulsive near degeneracies *J. Phys.* A **23** L655–7
[11] Berry M V 1984 Quantal phase factors accompanying adiabatic changes *Proc. R. Soc.* A **392** 45–57
[12] Simon B 1983 Holonomy, the quantum adiabatic theorem, and Berry's phase *Phys. Rev. Lett.* **51** 2167–70
[13] Berry M V and Shukla P 2018 Geometric phase curvature for random states *J. Phys.* A **51** 475101
[14] Berry M V and Shukla P 2020 Geometric phase curvature statistics *J. Stat. Phys.* (accepted) https://doi.org/10.1007/s10955-019-02400-6
[15] Mead C A and Truhlar D G 1979 On the determination of Born–Oppenheimer nuclear motion wave functions including complications due to conical intersections and identical nuclei *J. Chem. Phys.* **70** 2284–96
[16] Mead C A 1992 The geometric phase in molecular systems *Rev. Mod. Phys.* **64** 51–85
[17] Von Neumann J and Wigner E 1929 On the behavior of eigenvalues in adiabatic processes *Phys. Z.* **30** 467–70
[18] Walker P N and Wilkinson M 1995 Universal fluctuations of Chern integers *Phys. Rev. Lett.* **74** 4055–8
[19] Porter C E 1965 *Statistical Theories of Spectra: Fluctuations* (New York: Adademic Press)
[20] Wong R 1989 *Asymptotic Approximations to Integrals* (New York: Academic)